

# Three Dimensional Numerical Analysis of Underground Bifurcated Tunnel

Xianshan Liu · Yong Wang

Received: 12 October 2009 / Accepted: 28 January 2010 / Published online: 10 February 2010  
© Springer Science+Business Media B.V. 2010

**Abstract** As far as the bifurcated tunnel of underground engineering is concerned, it is usually used in the water conveyance system. Due to the complexity of underground rock masses and concrete lining, researches on mechanical characteristic and stability of the bifurcation tunnel have attracted more and more attention in the geotechnical field. In order to understand bifurcated tunnel in detail, three-dimensional (3D) numerical method is applied to solve the above key subjects by simulating a practical project. Furthermore, sub-model technology is applied to analyze the intersection position, corresponding deformation and stress results in the practical condition. Meanwhile, 3D excavation and support calculation under four conditions have been simulated based on 3D self-compiled code and Ansys software. In addition, the paper plays emphasis on the stress, displacement analysis considering different stress releasing ratio instead of rheological analysis, and the results corresponding with the fact indicate the feasibility of 3D elasto-visco-plastic code.

**Keywords** Bifurcated tunnel · Stability · 3D numerical method · Sub-model · Stress releasing ratio

## 1 Introduction

Bifurcated tunnel is usually applied in the underground engineering, but rock behavior at the intersection area of the main tunnel and branch tunnels is a complicated three-dimensional (3D) problem, so research on its mechanical characteristics plays an important role on understanding the tunnel conditions. Most of the previous studies on intersection area of the underground tunnel were conducted using elasticity theory. In recent years, due to rapid development of computer and modelling techniques, 3D numerical analysis was used more widely by researchers to solve the complex geological model, bifurcated part and structure, deformation and stress distribution, etc. (Wang and Wang 2003; Zhang and Li 2004; Bai and Huang 2000). Among all the numerical methods, Finite Element Method (FEM; Wang and Shao 2001; Gao et al. 2002) is more and more mature and useful in dealing with the continuous medium in the field of geotechnical engineering.

However, without good and real geological model, tunnel behavior especially for intersection area cannot be reflected practically. Thus, a series of corresponding commercial softwares are developed to solve preprocess, local refinement named sub-model technology (Gao et al. 2002) and post-process and so on. For example, Ansys software is popular universal software performing structure mechanics, thermal mechanics and fluid mechanics and so on.

---

X. Liu (✉) · Y. Wang  
Department of Rock Mechanics, College of Civil  
Engineering, Chongqing University, 400044 Chongqing,  
China  
e-mail: liuxianshan@163.com

Furthermore, it's so powerful to preprocess and post process especially graphic interfaces and interactive operation that simulation results are more accurate and practical. A case in point, Ansys can verify geometric shape, materials and boundary conditions through graph display before calculation, and also can output the simulation results by multiple ways such as color nephogram, contour and animation display.

Due to the complexity of the underground bifurcated tunnel, combining the convenience of Ansys software and the flexibility of self-compiled FEM code, a perfect elasto-visco-plastic method is performed to solve the tunnel named Wujiangdu tailrace bifurcation in China. According to the requirement of the practical project, the paper plays the emphasis on stress and displacement distribution analysis (Lazarus and Leblond 2002; Okazaki et al. 1998; Watts and Nilsen 2008; Fleming and Watts 2007) of the bifurcated tunnel and intersection area considering different stress releasing ratio (Healy and Riordan 2002) under different working conditions, which provides a reliable basis for structure design and stability assessment of the underground engineering.

## 2 Analysis theory of underground bifurcated tunnel

### 2.1 Anchor modeling

In order to better simulate the anchoring effect, two important methods, the anchor element method and equivalent continuum method are introduced in recent years. In this paper, the latter method is considered. The equivalent method is to get equivalent mechanical parameters after considering a large range of anchoring effect according to mathematical and mechanical theory. Based on in situ experiments and theoretical studies, we can conclude the equivalent anchoring effect by the following formula:

$$C_b = C \left( 1 + \eta \frac{\tau_b A_b}{S_a S_b} \right) \quad (1)$$

where  $C$ ,  $C_b$  is, respectively the cohesion of the surrounding rock before and after anchorage (Unit: MPa);  $\tau_b = (0.6\text{--}0.8) R_L$ ,  $R_L$  is design tensile strength

of the concrete (Unit: MPa);  $A_b$  is the anchor cross-sectional area (Unit:  $\text{cm}^2$ );  $S_a$ ,  $S_b$  is bolts spacing and row spacing (Unit: cm); and  $\eta$  is the experimental coefficient (range: 10/Mpa–15/Mpa).

### 2.2 Concrete elasto-plastic constitutive relations

Consider backfill grouting and great friction between the concrete and surrounding rocks of the tunnel project, two assumptions are made for the research: (1) no relative slip between the concrete lining and surrounding rocks considering the internal water pressure; (2) before the reinforced concrete cracking, both the concrete and bars are under good adhesive condition and have common deformation.

Therefore, we apply the E. Hognestad model in the tunnel project, the corresponding expression is given as follows. When

$$\sigma \leq 0.3f_c, \quad \sigma = E_c \varepsilon \quad (2)$$

when  $\sigma \geq 0.3f_c$ ,  $\varepsilon \leq \varepsilon_0$  (upward section)

$$\sigma = f_c \left( 2 \frac{\varepsilon}{\varepsilon_0} - \left( \frac{\varepsilon}{\varepsilon_0} \right)^2 \right) \quad (3)$$

when  $\sigma \geq 0.3f_c$ ,  $\varepsilon_0 \leq \varepsilon \leq \varepsilon_u$  (down section),

$$\sigma = f_c \left( 1 - 0.152 \left( \frac{\varepsilon - \varepsilon_0}{\varepsilon_u - \varepsilon_0} \right)^2 \right) \quad (4)$$

where  $E_c$  is the elastic modulus of the concrete;  $f_c$  is the peak strength, which denotes the ultimate compressive strength of the prism;  $\varepsilon_0 = 0.002$ , represents peak strain corresponding peak stress; and  $\varepsilon_u = 0.0038$ , is ultimate compressive strain.

## 3 Information about the underground bifurcated tunnel

### 3.1 Project introduction

The underground bifurcated tunnel is located in Wujiangdu in China. The water diverting system includes two bank-tower intakes and two diversion pipes, the diameter of the pipes is 7.0 m. And the tailrace water from the tailrace pipe diffuser (Watts and Nilsen 2008; Fleming and Watts 2007) in the main powerhouse passes through the branch tunnels

**Table 1** Mechanical parameters of supporting materials

Material	Bulk density (kN/m <sup>3</sup> )	Elastic modulus (GPa)	Poisson ratio	Compressive strength (MPa)	Tensile strength (MPa)
Anchor bolt	–	200	0.25	310	310
Spray-up concrete	25.0	22.0	0.20	32.5	5.0
Concrete (C25)	25.0	28.0	0.167	12.5	1.3

**Table 2** Mechanical parameters of surrounding rock masses

Material	Bulk density (kN/m <sup>3</sup> )	Elastic modulus (GPa)	Poisson ratio	Friction coefficient	Cohesion (c'; MPa)
Limestone	27.2	18	0.17	1.2	1.1
Shale	27.0	6	0.30	0.7	0.25
Weak intercalation layer				0.4	0.08
Fault F115 and shuttered zone		0.75	0.30	0.4	0.03

to the main tunnel, the section of the main tunnel is round, its diameter is 15.1 m, and the maximum span length is 30 m.

### 3.2 Material parameters

Mechanical parameters of support materials and surrounding rock masses are given by the following Tables 1 and 2.

### 3.3 Load and load combination

- (1) Normal operation condition (named condition A). The load combination is: Gravity stress field + Releasing load of surrounding rock masses after excavation + Support resistance + Structure weight + Internal water pressure + External water pressure \*0.15.
- (2) Backfill grouting condition (named condition B). Range of the backfill grouting is 120° and the pressure is 0.2 MPa. The load combination is: Gravity stress field + Releasing load of surrounding rock masses after excavation + Support resistance + Structure weight + Internal water pressure + Backfill grouting pressure.
- (3) Maintenance condition (named condition C). The load combination is: Gravity stress field + Releasing load of surrounding rock masses after excavation + Support resistance + Structure weight + Internal water pressure + External water pressure \*0.80.

- (4) Accidental condition (named condition D). The load combination is: Gravity stress field + Releasing load of surrounding rock masses after excavation + Support resistance + Structure weight + Internal water pressure + External water pressure \*0.20.

## 4 Numerical model and sub-model study

The calculation range of geological model: transverse size is 3 ~ 3.5 the main tunnel diameter. Boundary condition: normal constraint around the model and the bottom.

Constitutive model of all the materials is given as follows:

- (1) All the weak interlayers: multilayer model.
- (2) Anchor bolt: Von Mises yield criterion. The anchor is adhesive and passive which is simulated with equivalent model mentioned in Sect. 2.1.
- (3) Rock masses and faults: Drucker-Prager yield criterion.
- (4) Shale interlayer: Mohr–Coulomb yield criterion.
- (5) Spray-up concrete and concrete lining: linear elastic model.

The numerical models are given by the following Figs. 1, 2, 3. For the initial physical model, the element mesh of the intersection part is so coarse that the corresponding calculation results are not too accurate. Thus sub-model technology (Gao et al. 2002) is applied to solve the difficulty. The tech-

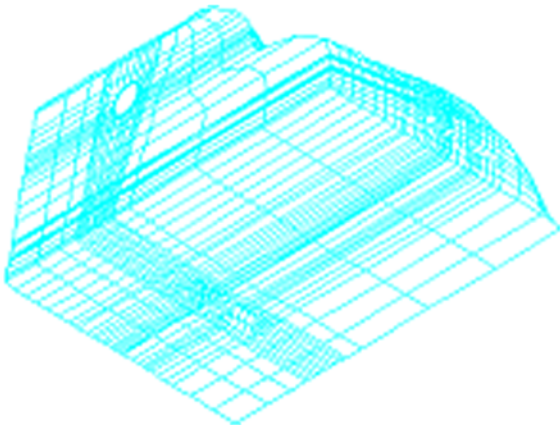


**Fig. 1** FEM numerical meshes of integral mode

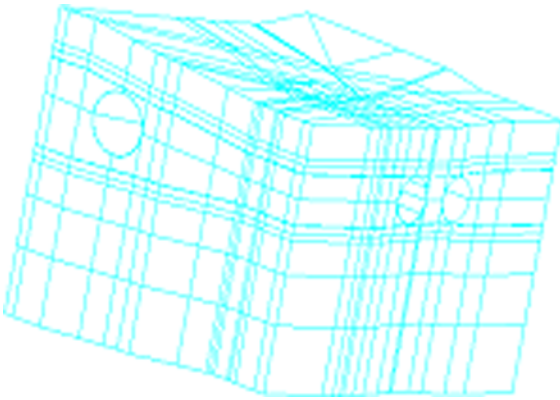


**Fig. 2** Detailed meshing of bifurcated tunnel

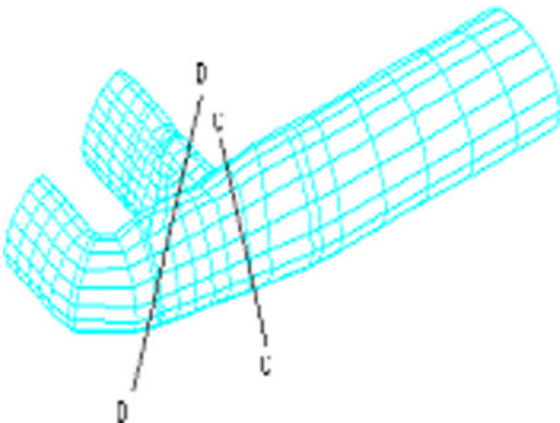


**Fig. 3** FEM meshing figure of bifurcated tunnel

nology (Wang and Shao 2001; Gao et al. 2002) is called cutting edge method or special edge method. The cut edge separated from the original coarse

model is sub-model's boundary. The original simulation results of the part are boundary constraint condition of sub-model. According to Saint–Venant theory, the sub-model technology may obtain accurate results if the intersection part is far from the stress concentration.

The analysis process includes the following steps:

Build the initial coarse meshing model.

Intercept the intersection part from original model as a sub-model and refine meshes.

Sub-model analysis: according to the final results of original model we can get the initial boundary condition of the sub-model. And analyze deformation and stress of the sub-model to obtain more precise results.

## 5 Results of analysis and discussion

Due to the absence of deformation-time curve, elasto-visco-plastic analysis is done based on different stress releasing ratio instead of rheologic analysis (Healy and Riordan 2002; Lazarus and Leblond 2002; Okazaki et al. 1998; Watts and Nilsen 2008; Fleming and Watts 2007.). Stress releasing ratio considers stress and load is proportional. Because the proportional ratio is related to practical experience, lithology, construction methods, support way and so on, the range of stress releasing ratio in the self-compiling elasto-visco-plastic program is supposed.

Case T1 and case T2 are considered. Case T1: suppose the stress releasing ratio 0.4:0.6 for the process of excavation and support. Case T2: suppose the stress releasing ratio 0.6:0.4 for the above process. The self-compiling program setting is as follows: set the initial excavation load  $P$ , and store the releasing load  $P_1$  (value is  $0.4P$  or  $0.6P$ ), and when supporting, add  $0.6P_1$  or  $0.4P_1$  to the anchor bolts and interact with the surrounding rock masses.

For the numerical analysis, two assumptions are used: (1) Full-face excavation; (2) Supporting parameters of two cases are constant. And four arrangements of anchor bolts are applied: (1) Arrange common mortar bolt  $\Phi 25$  in the branch tunnel, the length is 5,500 mm, the embedment depth in rock is 4,500 mm, and row spacing is 1,500 mm; (2) Arrange 5 rows pre-stressed bolts  $\Phi 32$  in the intersection part, the length is 12,000 mm, row spacing is 1,500 mm; (3) Arrange

**Table 3** Calculation results of two cases

Calculation Case		Case T1	Case T2
Maximal displacement of surrounding rock masses (mm)	Supporting stage	2.06	5.02
	Lining stage	3.79	5.51
Plastic zone of surrounding rock masses	Supporting stage	Located in the position of bifurcation, fault and shale, the range is relatively small	Located in the position of bifurcation, fault and shale, the range is $-20^\circ \sim 70^\circ, 150^\circ \sim 250^\circ$
	Lining stage	Located in the position of bifurcation, fault and shale, the range is relatively small	Located in the position of bifurcation, fault and shale, the range is $-45^\circ \sim 85^\circ, 140^\circ \sim 250^\circ$
Maximal stress of anchor bolt (Mpa)	Supporting stage	21.9	47.0
	Lining stage	46.0	53.1
Maximal lining stress (Mpa)	Lining stage	-5.45	-2.10

common bolt  $\Phi 32$  and  $\Phi 22$  in the transition of main and branch tunnel, the length is 7,500 and 4,500 mm, and the embedment depth in rock is 6,500 and 3,000 mm, respectively, and row spacing both is 1,500 mm; (4) Arrange common bolt  $\Phi 32$  and  $\Phi 22$  in the main tunnel, the length is 7,500 and 3,000 mm, embedment depth in rock is 6,500 and 3,000 mm, respectively, and row spacing both is 1,000 mm.

The supporting material named steel fiber shotcrete grade C25, the thickness is 1,200 mm in the branch tunnel, and the rest is 1,500 mm.

### 5.1 Calculation analysis of two cases

The results of two cases listed in Table 3.

- (1) Before supporting for case T1, the stress releasing ratio is so small that the maximal displacement is very small and there is no plastic zone. However, for case T2, due to the larger stress releasing ratio, the large maximal displacement is relatively larger and the plastic zone has appeared. Therefore, in order to make good use of self-support capacity and reduce the force of support structure, case T1 is difficult to satisfied the practical need. But for case T2, corresponding displacement distribution and plastic zone of surrounding rock masses is close to the practical state. In order to avoid the larger deformation of surrounding rock masses, the supporting time is not too late. According to the above analysis, case T2 is more suitable comparatively.
- (2) As for as supporting and lining stage is concerned, the stress of case T1 is lower in the one-time supporting stage, but the lining stress is very high after finishing lining because the higher stress releasing ratio is considered in the stage. For case T2, suppose the larger stress releasing ratio in the early stage, supporting stress is higher and the lining stress is lower comparatively. Though supporting stress of cases is different, the value is greatly lower than the design strength of lining materials, which indicates that the supporting parameters may be optimized.
- (3) The surrounding rocks deform toward the tunnel due to the load releasing when tunneling. According to the numerical simulation results, vertical displacement also reaches the maximum. And the displacement of the surrounding rocks close to the mountain is relatively larger.
- (4) According to the numerical analysis shown in the Table 3, there exists shear yield region for the surrounding rocks, most area of which is mainly in the area of fault, intersection and shale layer. The detailed information is explained as: (a) for intersection area, shear yield region mainly exists in the side-wall rocks and the surrounding rocks of the intersection part, but there is no shear yield region on the top of the tunnel. (b) As for the fault in the intersection position, fault is yielded in the top and bottom of the tunnel. (c) For the shale region, the maximum plastic yield region is in



the limestone region and the tunnel is nearly yielded. However, plastic yield region is narrowing gradually far away from the limestone region because the difference of elastic modulus of two rocks is very large. Furthermore, the deformation of shale region is enlarged and the shear stress is appeared because larger deformation of the shale is constrained by the limestone, but the shear effect decreases gradually far away from the limestone area.

### 5.2 Analysis of concrete lining

According to the numerical results of case T1 and case T2, we can arrange total displacement and first principal stress contour of lining section (thickness is 1.5 and 1.2 m). As far as different working conditions mentioned above are concerned, the figures of displacement contour (unit: m) and stress contour (unit: MPa) of the intersection area D–D are showed by the following Figs. 4, 5, 6, 7, 8, 9, 10, 11, 12, 13, 14 and 15.

The displacement and stress contour is symmetric approximately according to the figures mentioned above, but maximal and minimal value appear neither at the top of section nor at the bottom of section of the intersection area because the shape of bifurcated tunnels is asymmetry and complicated mechanical characteristics of the surrounding rocks and faults directly affect the stress distribution. Furthermore, we can find that the first principal stress appears on the left-bottom of bifurcated tunnel and all stress is compressive. As far as the normal operation

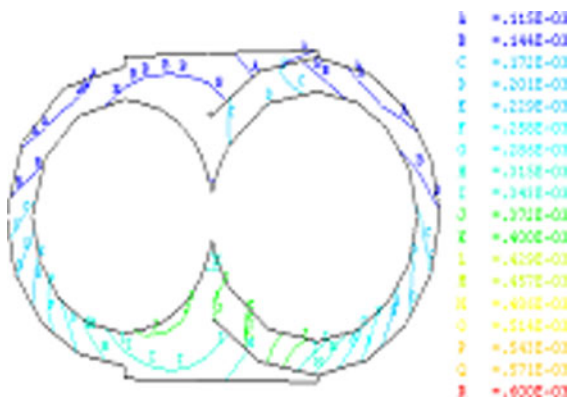


**Fig. 4** Displacement contour in lining section D–D (T1, normal condition)

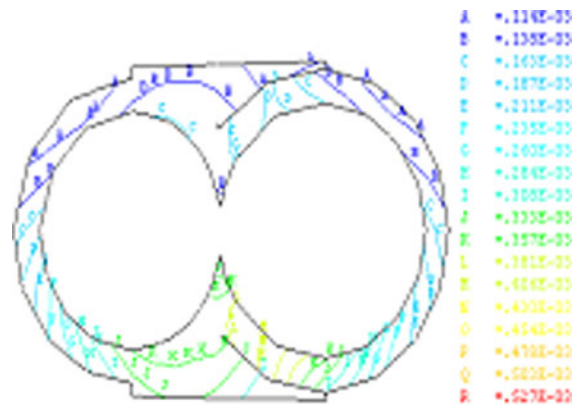


**Fig. 5** Displacement contour in lining section D–D (T2, normal condition)

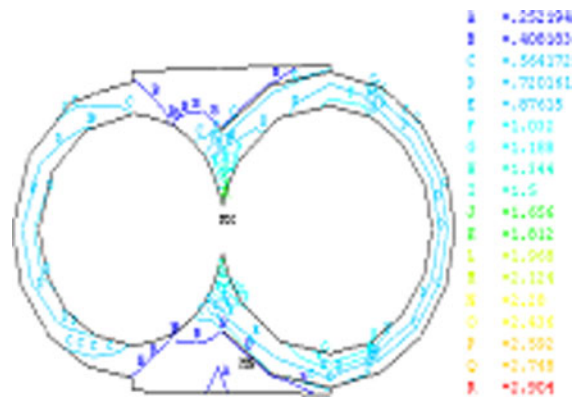


**Fig. 6** First principle stress contour in lining section D–D (T1, normal condition)

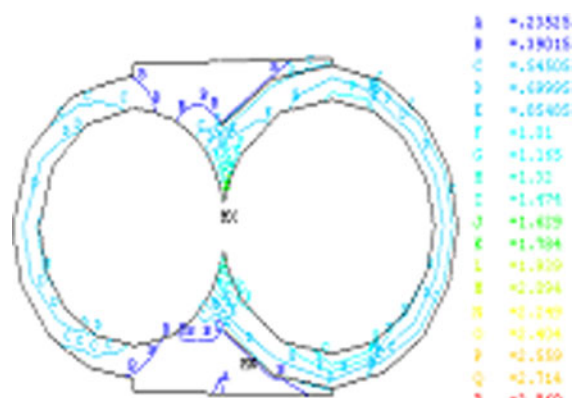


**Fig. 7** First principle stress contour in lining section D–D (T2, normal condition)

condition is concerned, there is no change for the maximal stress of anchor bolts, but the zone of maximal stress change greatly, which illustrates that

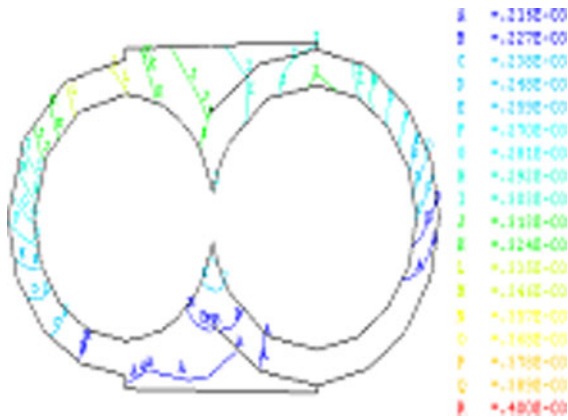


**Fig. 8** Displacement contour in lining section D–D (T1, Backfill grouping condition)

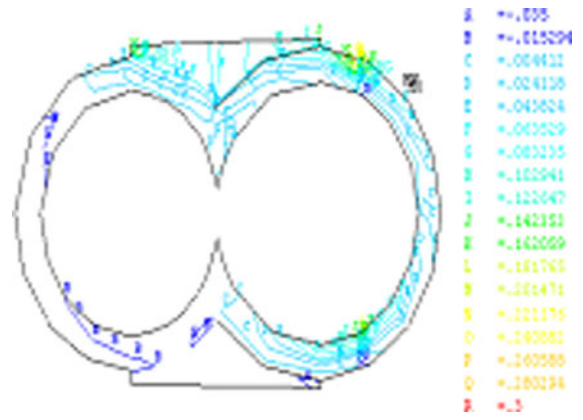


**Fig. 11** First principle stress contour in lining section D–D (T2, Backfill grouping condition)

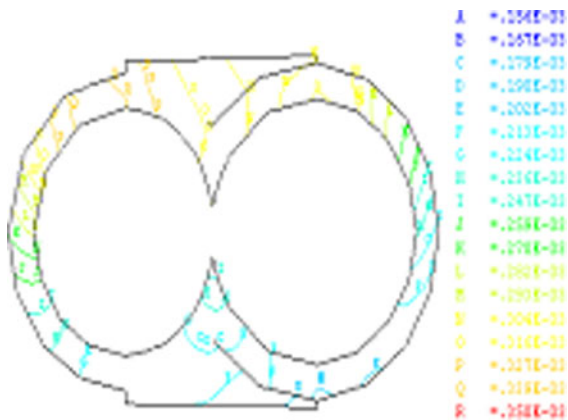


**Fig. 9** Displacement contour in lining section D–D (T2, Backfill grouping condition)

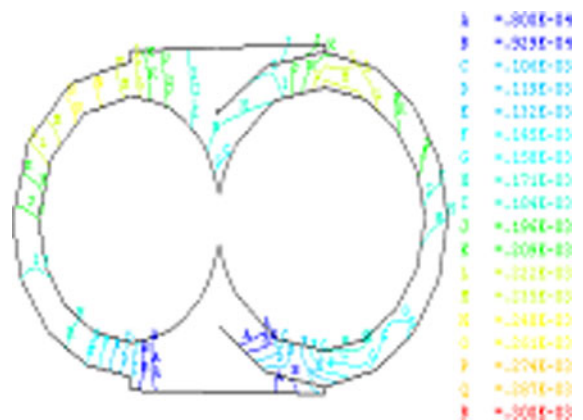


**Fig. 12** Displacement contour in lining section D–D (T1, maintenance condition)

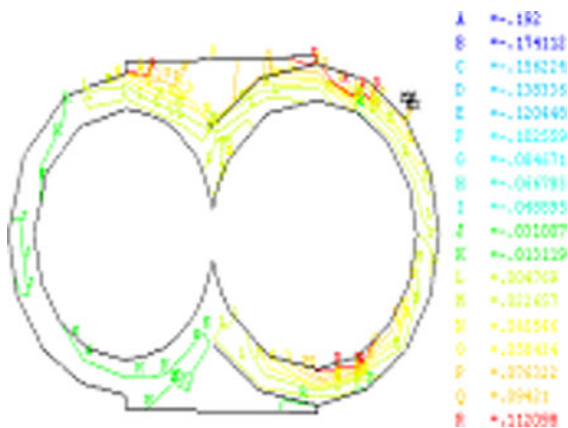


**Fig. 10** First principle stress contour in lining section D–D (T1, Backfill grouping condition)

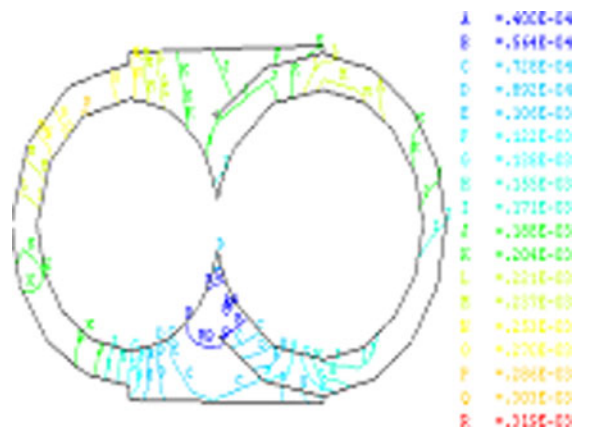


**Fig. 13** Displacement contour in lining section D–D (T2, maintenance condition)

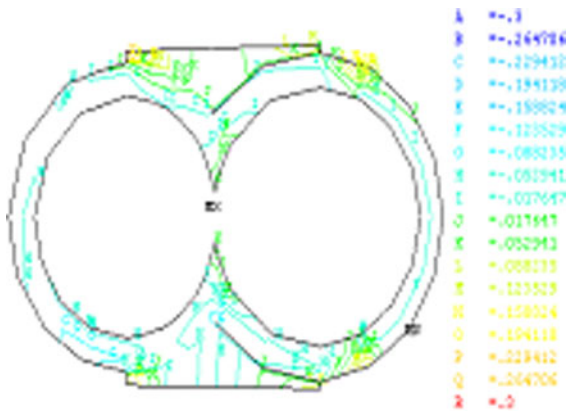


**Fig. 14** First principle stress contour in lining section D–D (T1, maintenance condition)

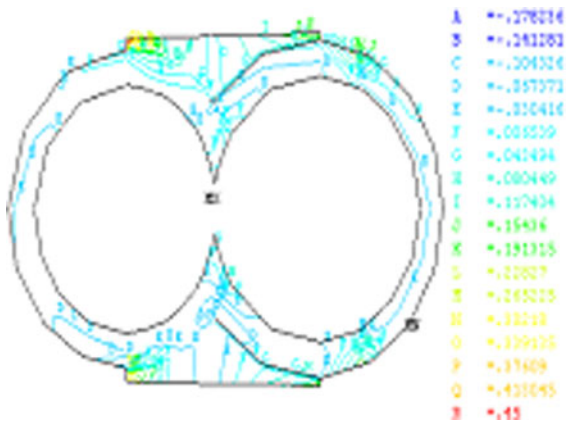


**Fig. 15** First principle stress contour in lining section D–D (T2, maintenance condition)

subsequent load applied on the concrete lining cannot affect the stress values of anchor bolts. But the range of plastic zone varies greatly.

On the other hand, water pressure can unload the surrounding rocks to make the yield rocks come back to elastic condition. As far as internal water pressure is concerned, water pressure downwards is more than upwards, water pressure upwards only affects deformation and stress of surrounding rocks close to tunnel. Therefore, the mountain cannot be destroyed by the internal water pressure.

According to the results shown in the tables and figures, we can include that the pre-process and self-compiled elasto-visco-plastic code are accurate, which also illuminates that it's applicable to apply the stress releasing ratio to the elasto-visco-plastic analysis in place of rheologic analysis.

In the process of lining, take case T1 and T2 under all work conditions mentioned above into account, plastic area of surrounding rock masses is basically identical according to the simulation results. (a) There is little change for the plastic region under backfill grouting condition. (b) And under the operation condition, because of water pressure being outward which make the surrounding rocks unload and the yielded rocks may partly be back to the elastic condition. And as for the internal water pressure, the downward pressure in the lining is larger than the upward pressure, and the upward pressure only affects the rocks near the tunnel perimeter. Therefore, there is little effect for the surrounding rocks far away from the tunnel perimeter and the slope cannot lose stability due to the internal water pressure. (c) As for the maintenance condition, because the deformation to the tunnel is identical with that of tunneling, plastic area of the surrounding rocks is enlarged, which is unfavorable to the engineering stability. Therefore, the condition can be as controlled condition for the surrounding rocks near the tunnel perimeter.

If considering the maximum tensile stress of two cases, the value of all conditions is approximate, which demonstrates anchor application time cannot greatly affect the concrete lining stress during the later period.

## 6 Conclusions

In this paper, underground bifurcated tunnel was simulated by Ansys software and 3D elasto-viscoplastic self-compiled code. The results show that Ansys software is powerful to deal with complex physical model and post-process using colorful nephograph, contour and animation display and so on. Meanwhile, the results indicate that the key calculation code can reflect the practical condition of the project.

- (1) Sub-model technology is applied in the pre-process, which can make the deformation and stress distribution of the bifurcated tunnel more precise because sub-model can refine the local complex model to get satisfied values.
- (2) The results according with the practical condition illuminate that it's applicable and reliable



for the elasto-visco-plastic analysis in place of rheologic analysis considering different stress releasing ratio.

- (3) Consider no releasing load after lining in the later period, anchored time cannot greatly affect the lining stress and may be neglected. And the backfill grouting condition has little effect on the deformation and stress of the tunnel lining and surrounding rocks, but the maintenance condition mainly control the stability of the surrounding rocks, on the other hand, the operating condition and accidental condition mainly control the deformation and stress of the tunnel lining.
- (4) Internal and external water pressure of the lining is considered as surface pressure regardless of the lining's permeability. Thus, how to accurately simulate seepage effect need advanced study.

## References

- Bai MZ, Huang GM (2000) 3-Dimensional finite element analysis about stability of surrounding rock mass of giant underground cavity. *West Explor Eng* 62(1) 63–65 (in Chinese)
- Fleming R, Watts C (2007) Breakthrough outage at the second Manapouri tailrace tunnel project, New Zealand. In: *Proceedings rapid excavation and tunneling conference, rapid excavation and tunneling conference*. pp 1262–1273
- Gao YD, Yang JM, Wang JX (2002) Applications of Ansys's submodel technique. *J Baotou Univ Iron Steel Technol* (12):340–342 (in Chinese)
- Healy C, Riordan C (2002) High bifurcation of median nerve at the wrist causing common digital nerve injury in carpal tunnel release[J]. *J Hand Surg* 27(6):580–582
- Lazarus V, Leblond JB (2002) In-plane perturbation of the tunnel-crack under shear loading I: bifurcation and stability of the straight configuration of the front[J]. *Int J Solids Struc* 39:4421–4436
- Okazaki H, Nakano D, Kawase T (1998) Chaotic and bifurcation behavior in an autonomous flip-flop circuit used by piecewise linear tunnel diodes. *IEEE Int Symp Circuits Syst* 1–6: 291–297
- Wang XC, Shao M (2001) *Basic theory of FEM and corresponding numerical methods*. TsingHua publishing company, Beijing, China
- Wang Z, Wang JQ (2003) Finite element analysis of Wanjiashai water transmission tunnel excavation and service. *Journal of Southeast University* 19(4):387–391 (in Chinese)
- Watts CR, Nilsen B (2008) Field application of NTH fracture classification at the second manapouri tailrace tunnel, New Zealand. In: *North American tunneling 2008 proceedings, 9th North American tunneling conference*. pp 236–242
- Zhang ZQ, Li N (2004) 3-D FEM analysis for excavation sequence of large scale power tunnels. *Journal of Hydroelectric Engineering* 23(6):83–87 (in Chinese)